International Journal of General Medicine

Dovepress
Taylor & Francis Group

Open Access Full Text Article

ORIGINAL RESEARCH

Machine Learning-Derived Diverse Regulated Cell Death Patterns for Therapeutic Target Identification in Glaucoma

Qianxue Mou[1], Gaigai Li[2], Sifei Xiang[1], Yin Zhao[1], Ke Yao[1]

[1]Department of Ophthalmology, Tongji Hospital, Tongji Medical College, Huazhong University of Science and Technology, Wuhan, 430030, People's Republic of China; [2]Department of Neurology, Tongji Hospital, Tongji Medical College, Huazhong University of Science and Technology, Wuhan, 430030, People's Republic of China

Correspondence: Ke Yao, Department of Ophthalmology, Tongji Hospital, Tongji Medical College, Huazhong University of Science and Technology, Wuhan, 430030, People's Republic of China, Tel +8618771053657, Email keyao1106@hust.edu.cn

International Journal of General Medicine downloaded from https://www.dovepress.com/
For personal use only.

Purpose: Glaucoma is the leading cause of irreversible vision loss worldwide. We aimed to uncover the molecular mechanisms and regulatory networks of hub genes in human glaucoma to identify promising targets for detection and treatment.

Methods: We obtained GSE758, GSE2378, and GSE9944 datasets from the Gene Expression Omnibus database. The list of genes linked to regulated cell death (RCD) was obtained from a previous study. RCD-related differentially expressed genes (DEGs) were identified in patients with glaucoma and controls. Weighted Gene Co-Expression Network Analysis (WGCNA) and machine learning algorithms were used to identify hub genes. Gene set enrichment analysis (GSEA) was used to explore signaling pathways enriched by hub genes, and molecular docking analysis was performed to identify the gene-drug network of hub genes for potential treatment. Immunofluorescence was used to reveal the expression levels of hub genes in glaucomatous mice and controls.

Results: This study identified 358 RCD-related DEGs that distinguished healthy individuals from glaucoma patients and underscored the pivotal involvement of the immune response in human glaucoma pathogenesis. We systematically identified 33 hub genes, including PLEC, DLGAP4, Glycosylphosphatidylinositol (GPI), etc. that demonstrated significant diagnostic or treatment potential for glaucoma. The cytoskeletal regulator PLEC has emerged as a promising candidate gene associated with glaucomatous neurodegeneration with possible acting drugs.

Conclusion: We constructed a machine-learning-driven analytical framework based on diverse RCD patterns to refine molecular subtypes and druggable genes. These findings may provide novel targets for glaucoma detection and treatment.

Keywords: retinal ganglion cell, WGCNA, machine learning, immune cell infiltration

Introduction

Glaucoma is the primary cause of irreversible vision loss worldwide, and is estimated to affect 111.8 million people by 2040.[1] It is a neurodegenerative disease, characterized by progressive degeneration of retinal ganglion cells (RGCs) and thinning of the retinal nerve fiber layer, finally culminating in irreversible visual field loss.[2,3] The pathophysiology of RGC death involves interrelated mechanisms including oxidative stress, glial cell activation, and mitochondrial dysfunction. Thus, the development of neuroprotective strategies targeting these pathways has emerged as a crucial therapeutic approach to preserve residual visual function in glaucoma patients.[4]

Cell death may occur in multiple forms in response to different stresses.[5] It can be divided into accidental cell death (ACD) and regulated cell death (RCD) based on functional aspects.[6] RCD involves precise signaling cascades, including recognition, triggering, execution, and other effector molecules, and produces a signaling cascade reaction. It has unique biochemical, functional, and immunological consequences.[5,7] Under physiological conditions, RCD is also known as programmed cell death (PCD). The most common RCD pattern is apoptosis. Many forms of nonapoptotic RCD have been identified, including necroptosis, pyroptosis, ferroptosis, entotic cell death, netotic cell death, parthanatos,

Received: 16 July 2025
Accepted: 27 November 2025
Published: 4 December 2025

© 2025 Mou et al. This work is published and licensed by Dove Medical Press Limited. The full terms of this license are available at https://www.dovepress.com/terms.php and incorporate the Creative Commons Attribution – Non Commercial (unported, v4.0) License (http://creativecommons.org/licenses/by-nc/4.0/). By accessing the work you hereby accept the Terms. Non-commercial uses of the work are permitted without any further permission from Dove Medical Press Limited, provided the work is properly attributed. For permission for commercial use of this work, please see paragraphs 4.2 and 5 of our Terms (https://www.dovepress.com/terms.php).

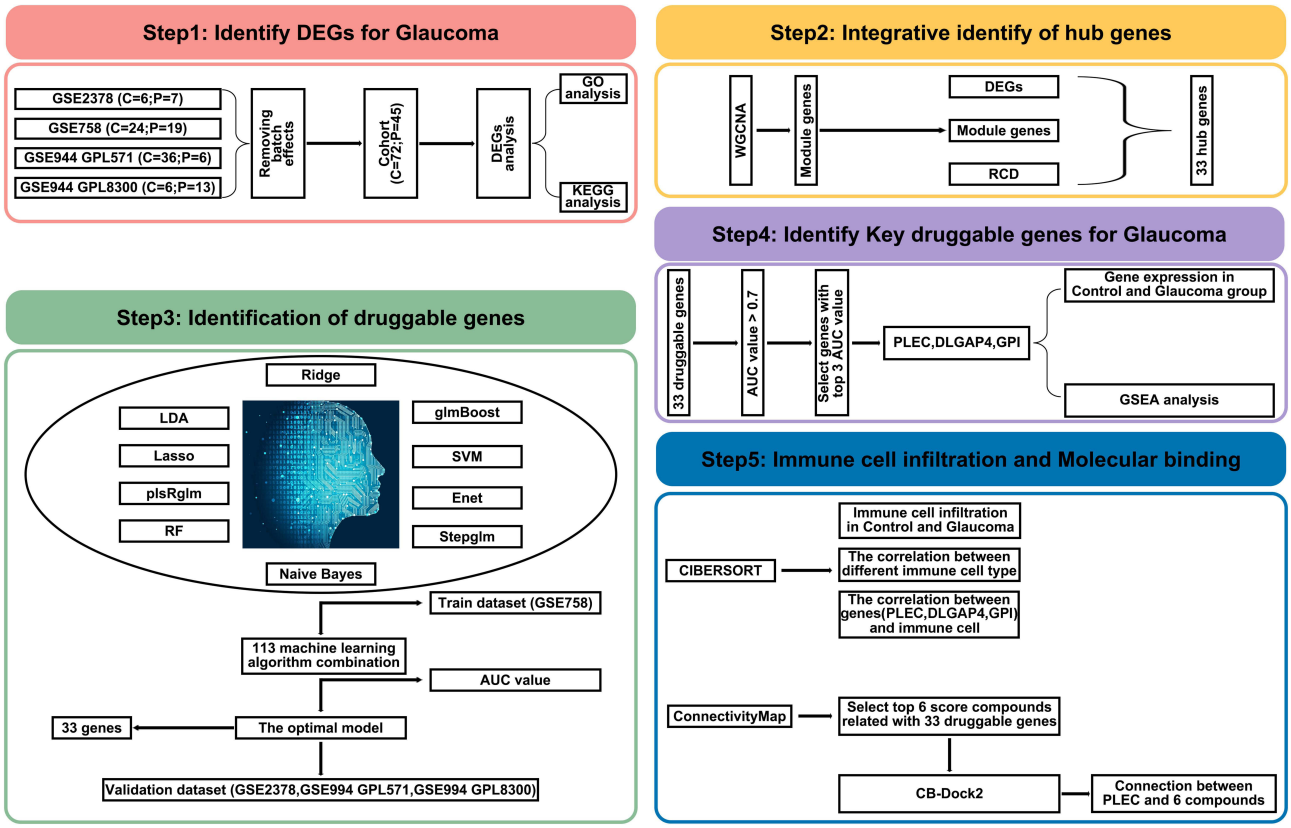

Figure 1 The flow diagram of the study. P represents the glaucoma patient, C represents the control.

lysosome-dependent cell death, autophagy-dependent cell death, alkaliptosis, and oxeiptosis etc.[5] Researchers have defined a network of 7460 RCD-related genes by developing a bioinformatics and in vivo discovery pipeline, providing researchers with an opportunity to reveal their role in tumor recurrence and metastasis.[8,9] Many studies have shown extensive crosstalk among different cell death pathways, such as PANoptosis, an inflammatory RCD pathway.[10–12] The roles of RCD and crosstalk in glaucoma have attracted extensive attention.[13,14] A recent study verified that inhibiting multiple forms of cell death optimizes ganglion cell survival after retinal ischemia-reperfusion injury.[15] Thus, it may be a new direction for future research on glaucoma therapeutic approaches to focus on crosstalk between different RCD pathways.

Numerous experimental studies using animal models of glaucoma have been conducted to develop neuroprotective therapeutics. However, whether these strategies are applicable to glaucoma in humans remains unclear. In this study, we sought to delineate the genetic risk profile of human glaucoma through systematic integration of three independent datasets following rigorous batch-effect correction and normalization (steps are shown in Figure 1). By leveraging the established list of RCD-related genes in patients,[9] differentially expressed genes (DEGs) and hub genes were identified via integrative analysis combined with weighted correlation network analysis (WGCNA). Comprehensive analyses of immune cell infiltration patterns in glaucoma patients and structure-based molecular docking analyses were performed. Our findings highlight candidate genes that may serve as reliable diagnostic biomarkers or potential therapeutic targets to develop innovative cellular and genetic therapies for glaucoma management.

Materials and Methods

Dataset Download and Differential Analysis

The datasets used in this study were obtained from the Gene Expression Omnibus (GEO) database, including the GSE2378 (GPL8300), GSE758 (GPL8300), GSE9944 (GPL571 and GPL8300). These datasets comprised sample

information from 72 non-glaucoma patients and 45 glaucoma patients, with all samples derived from the optic nerve head. By performing microarray information annotation and gene symbol conversion in the sangerbox database (http://sangerbox.com/login.html), gene expression data were read and converted into matrix format for easier manipulation and analysis. From this matrix, we extracted relevant expression data for further processing. Batch correction techniques have been applied to ensure the data integrity.[9] This step was crucial for eliminating errors introduced by the experimental batches, technical differences, or other systematic biases. After obtaining the processed expression matrix, we examined the data distribution characteristics to determine whether logarithmic transformation (log2) was necessary to stabilize the variance and improve data distribution, thereby ensuring the accuracy and analyzability of the gene expression data. DEGs were identified with a criterion of corrected P-values < 0.05 and a 1-fold difference (|LogFC| > 0.585) using the Limma package from R Bioconductor.

Functional Enrichment Analysis of DEGs

To investigate the functional roles of the identified DEGs in biological pathways, we performed Gene Ontology (GO) and Kyoto Encyclopedia of Genes and Genomes (KEGG) enrichment analyses using the enrichGO and enrichKEGG functions (clusterProfiler package, R/Bioconductor). We set a criterion with q-values less than 0.05, to capture GO and KEGG entries. To visually present the enrichment analysis results and the relationships between genes and entries, bar charts were created (https://hiplot.com.cn) to display the gene proportions of the enriched pathways.

WGCNA

WGCNA is a bioinformatics method that uses high-throughput gene expression data to construct co-expression networks.[16] In our study, WGCNA was performed using the WGCNA R package to identify the glaucoma-associated gene modules. Pairwise Pearson's coefficients were used to assess the weighted co-expression relationships between all the genes to produce an adjacency matrix. The least value for which the scale-free topology fit $R^2 > 0.75$ was chosen as the soft-threshold power. Pearson coefficients were produced for all paired genes; thus, the co-expression matrix was rendered into an adjacency matrix using a soft-threshold power. Soft-threshold power was selected based on a standard scale-free distribution. Scale-free co-expression networks were created with 30 genes as the minimal module size and 0.25 as the dendrogram cut height for module merging. A soft threshold is used to ensure a scale-free network. Genes with high correlations were clustered into the same module after the co-expression network formation.

Machine-Learning to Screen Out Druggable Genes

The GSE758 dataset was designated as the training cohort for feature selection and model development, whereas the GSE994 and GSE2378 datasets served as independent validation cohorts. A comprehensive evaluation of 75 machine-learning algorithms was performed to determine the optimal model for glaucoma prediction using AUC values.[8,17] The top three hub genes with the largest AUC were selected as therapeutic candidates.

Expression Level and GSEA Analysis of Co-Expressed Gene Sets for Hub Genes

Differential expression patterns of the top-ranked hub genes between glaucoma patients and non-glaucoma controls were quantified using boxplot visualization. GSEA was subsequently performed using the clusterProfiler R packages to identify molecular pathways significantly enriched in the high- and low-expression groups, with a threshold of $P < 0.05$.[8,18]

Molecular Docking

The top3-ranked hub genes were selected as glaucoma druggable gene sets, and the top six score compounds related to the glaucoma druggable gene set were selected using Clue (https://clue.io/query). The structure of the plectin protein encoded by the *PLEC* using RSCB PDB (https://www.rcsb.org/) and the molecular structures of the six compounds were also obtained using PubChem (https://pubchem.ncbi.nlm.nih.gov/). A molecular docking graph using CB-Dock2 (https://cadd.labshare.cn/cb-dock2/index.php) was presented.

Immune Cell Infiltration Analysis

To characterize immune microenvironment alterations in glaucoma, we performed immune cell infiltration analysis using the CIBERSORT algorithm and differential analysis.[17,19] After the calculation, the results were filtered, retaining only immune cell types with P-values of < 0.05. To further understand the relationship between the infiltration of these different types of immune cells, we used Pearson's correlation coefficient to identify correlations among the differentially expressed immune cell types. Additionally, the geoML26.immuneCor.R package was used to determine the correlation between identified druggable genes and immune cells.

Animals

All animal feeding and experimental procedures were approved by the Institutional Animal Research Committee of Tongji Medical Center and were conducted in compliance with the Guide for the Care and Use of Laboratory Animals published by the National Institutes of Health, Bethesda, Maryland, USA. Wild-type C57BL/6J mice and DBA/2J mice were obtained from Shulaibao (Wuhan) Biotechnology Co., Ltd. 10-month-old DBA/2J mice, which experienced spontaneous elevation in intraocular pressure, were used as glaucoma mice model in this study. C57BL/6J mice of the same age were used as the controls.

Tissue Preparation

After sacrifice by CO_2, mice eyeballs were harvested and immersed in freshly prepared 4% paraformaldehyde for 24 h at 4°C. Paraffin embedding was performed with precise orientation to ensure sections (4μm thickness) contained the optic nerve head (ONH) region, cut perpendicular to the corneal-optic nerve axis. Before immunofluorescence staining, the sections were dewaxed and immersed in trisodium citrate solution (pH = 6.0) for microwave antigen retrieval for 20 min.

Immunofluorescence

Following antigen retrieval, sections were blocked with 10% donkey serum for 1 h. Tissue sections were then incubated with diluted (1:1000) primary antibodies (anti-PLEC, 29170-1-AP, Proteintech; Tuj1, 801202, BioLegend) overnight at 4°C, followed by incubation with diluted (1:1000) secondary antibodies (Goat Anti-Mouse IgG H&L-Alexa Fluor 488, abcam, ab150113; Goat Anti-Rabbit IgG H&L-Alexa Fluor 647, abcam, ab150079) for 2 h at room temperature. Fluorescence microscopy (OLYMPUS BX51) at 20× magnification was used to acquire images of retinal sections.

Statistical Analysis

Statistical analyses were performed using GraphPad Prism software (version 10.0) to compare the two groups. $P<0.05$ was considered statistically significant.

Results

Identification of DEGs and RCD-Related DEGs Between Glaucoma Patients and Controls

The GEO datasets GSE758 (GPL8300), GSE2378 (GPL8300), and GSE9944 (GPL571 and GPL8300) were included in our analysis. Samples from non-glaucoma and glaucoma patients were obtained from the optic nerve heads. First, we removed batch effects from these datasets. The datasets were then combined as described in the Methods section (Figure 2A and B). In total, 637 DEGs were identified between the glaucoma and non-glaucoma groups comprising 341 upregulated and 296 downregulated genes. The magnitudes of differential expression for significant DEGs ($P < 0.05$, $|\text{fold change}| > 0.585$) are presented as a heatmap (Figure 2C) and a volcano map (Figure 2D), with additional details provided in Supplementary Table 1. GO and KEGG pathway analyses allowed for molecular function and signal pathway annotation of dysregulated genes. Our results indicated that these DEGs were predominantly enriched in GO CC terms "focal adhesion", "cell substrate junction" and "endocytic vesicle" MF terms "structural constituent of cytoskeleton", "electron transfer activity" and "growth factor binding" and BP terms "viral process", "viral life cycle" and "protein

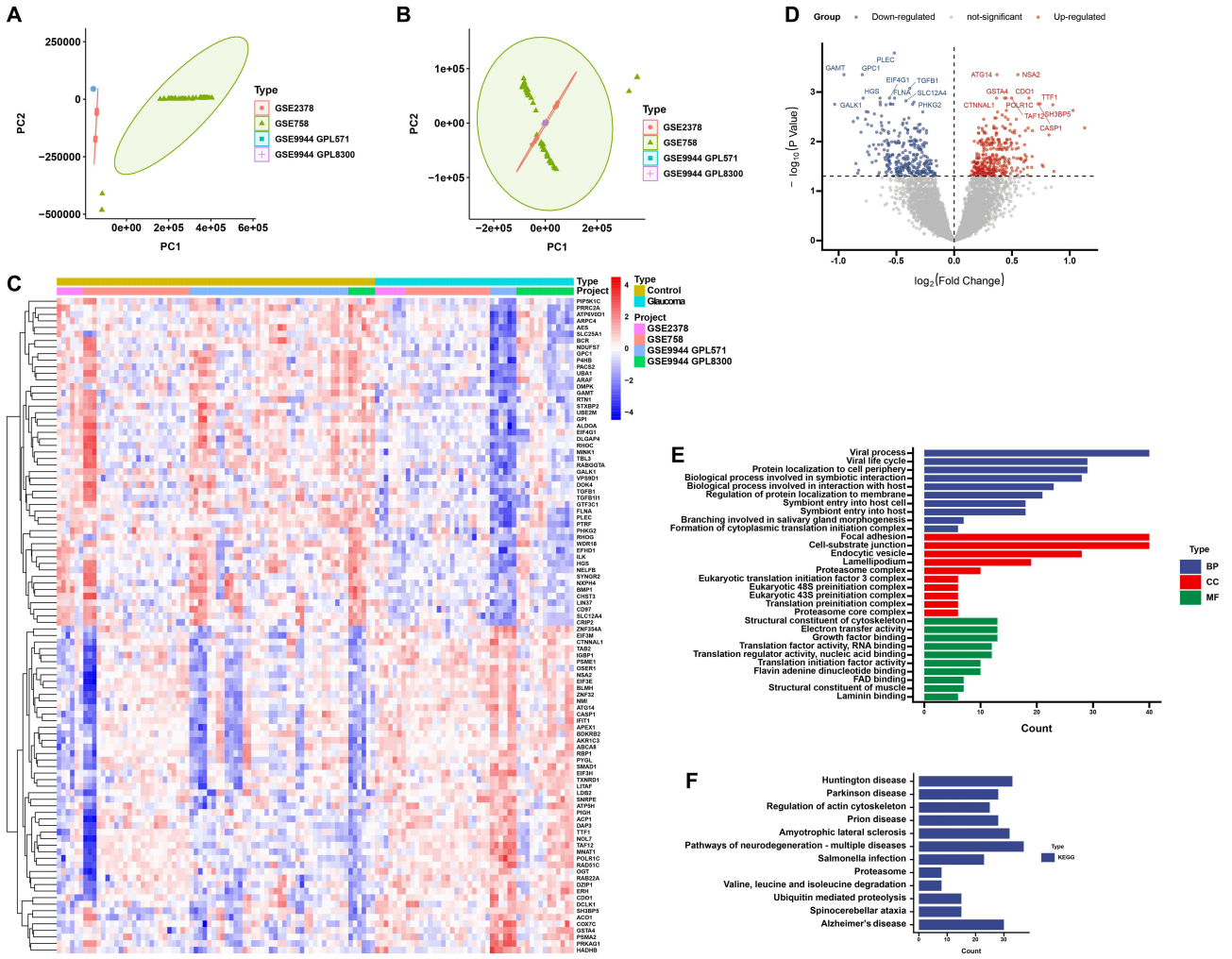

Figure 2 Differential expression genes (DEGs) analysis in glaucoma and non-glaucoma group. (**A** and **B**) Batch effects: before (**A**) and after (**B**); (**C**) Heatmap of DEGs between glaucoma and non-glaucoma group; (**D**) Volcano plot of up-regulated and down-regulated gene in glaucoma group; (**E**) GO enrichment analysis of DEGs; (**F**) KEGG enrichment analysis of DEGs.

localization to cell periphery" (Figure 2E). The KEGG pathway analysis indicated that 12 pathways were associated with DEGs, which mainly enriched in "regulation of actin cytoskeleton", and "neurodegenerative diseases" (Figure 2F).

To delineate glaucoma-associated genes intersecting RCD pathways, these DEGs were searched against the 7460 genes in Supplementary Table 2 for RCD genes,[8,9] yielding a total of 358 potential glaucoma-RCD interactions or crosstalk genes. The magnitudes of differential expression for significant RCD-related DEGs ($P < 0.05$, |fold change| > 0.585) are shown as a volcano map and a heatmap (Figure 3A and B) (details in Supplementary Table 3). The GO terms and KEGG pathways are shown in the diagram (Figure 3C and D).

WGCNA in Glaucoma

Glaucoma-related co-expressed gene modules were identified using WGCNA in R. First, the hclust function was used to analyze the samples. No outlier samples were found in the hierarchical clustering of samples (Figure 4A). The gene expression network was identified as a scale-free network when the soft threshold β was set to 8, achieving an R^2 value of 0.80 (Figure 4B), indicating a strong fit to the scale-free topology. The genes in glaucoma were analyzed by clustering and different gene modules, which are displayed in different colors. Thirteen gene modules were identified (Figure 4C and D). A Pearson correlation heatmap of module features with glaucoma was then generated to evaluate the associations between the modules and disease phenotypes (Figure 4E). The results revealed that the tan module had the strongest

https://doi.org/10.2147/IJGM.S545553

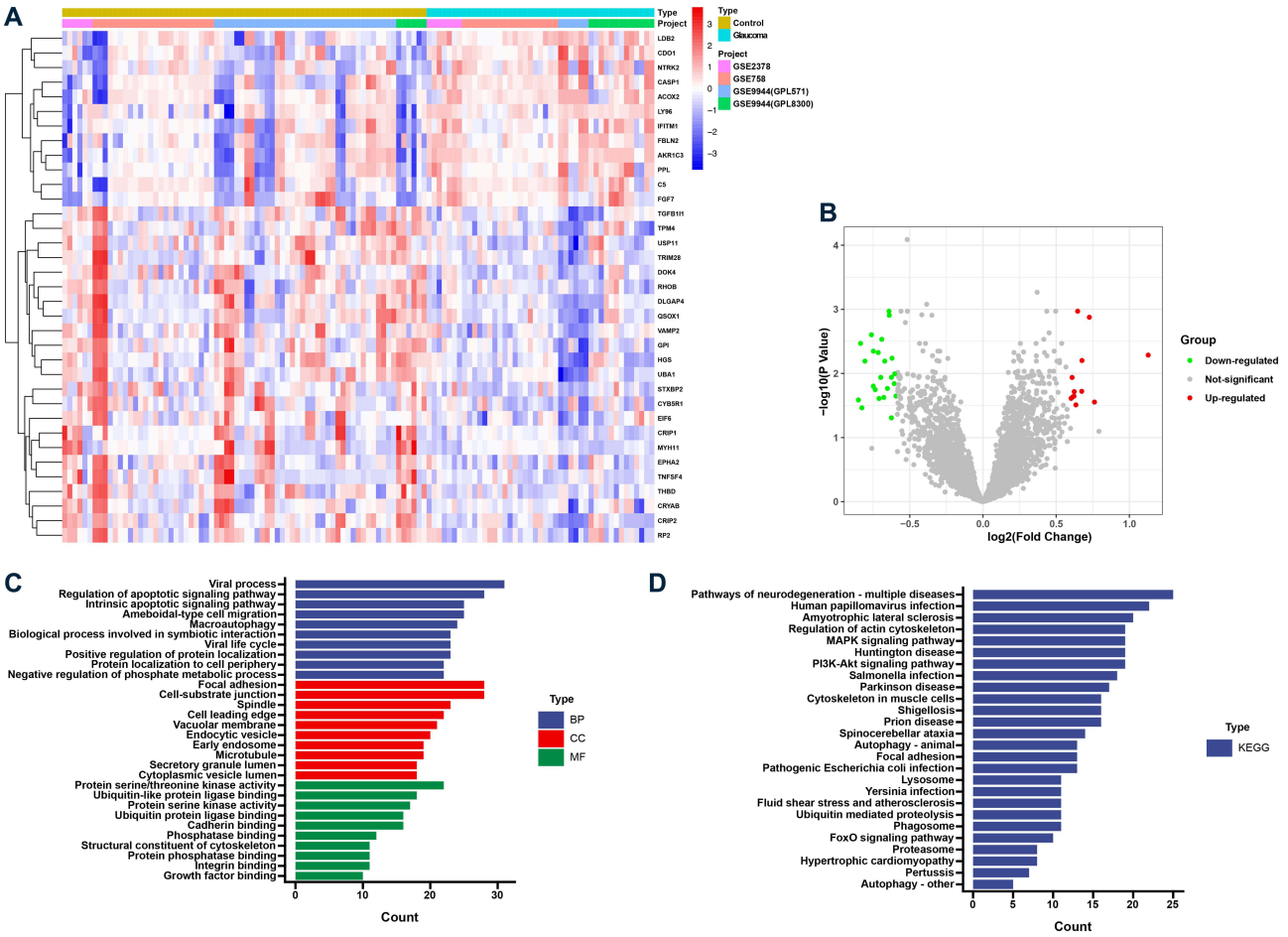

Figure 3 Regulated cell death (RCD) related-DEGs between glaucoma and non-glaucoma group. (**A**) Heatmap of differentially expressed RCD genes in glaucoma patients and non-glaucoma patients; (**B**) Volcano plot of up-regulated and down-regulated RCD genes in glaucoma patients; (**C**) GO enrichment analysis of RCD-related DEGs; (**D**) KEGG enrichment analysis of RCD-related DEGs.

correlation with glaucoma (r=0.37, p=4e-5). Additionally, correlation analysis of the tan module genes with glaucoma features was performed, and we discovered a remarkable correlation between them (Figure 4F).

We performed GO and KEGG pathway analyses of genes in the tan module. The genes were primarily enriched in the GO terms "actin filament organization" (BP), "focal adhesion" (CC), and "cadherin binding" (MF) (Figure 4G). The top KEGG pathways enriched include "Ras signaling pathway", "motor proteins", and "sphingolipid signaling pathway" (Figure 4H).

Hub Genes and Machine-Learning to Screen Out Candidates for Detection or Treatment

Hub genes refer to highly connected genes in a co-expression or protein-protein interaction network, playing a central regulatory role in biological processes.[16–18] We extracted genes from the tan module, RCD genes, and DEGs between glaucoma patients and controls, and presented them in a Venn diagram (Figure 5A). A total of 33 overlapping genes, including PLEC, GPC1, EIF4G1, and GALK1 etc., which are listed in Supplementary Table 4.

To further explore the 33 hub gene features, machine learning algorithms were used to screen for potential predictors. Intriguingly, the ridge regression model emerged as the most prominent model, with the highest average AUC (0.889) among all artificial intelligence algorithms (Figure 5B). To evaluate the diagnostic effectiveness of the cohort, we employed receiver operating characteristic (ROC) curve analysis, which demonstrated the performance of the ridge regression method. The AUC, which represents the area under the ROC curve, was determined to be 0.846 in the training

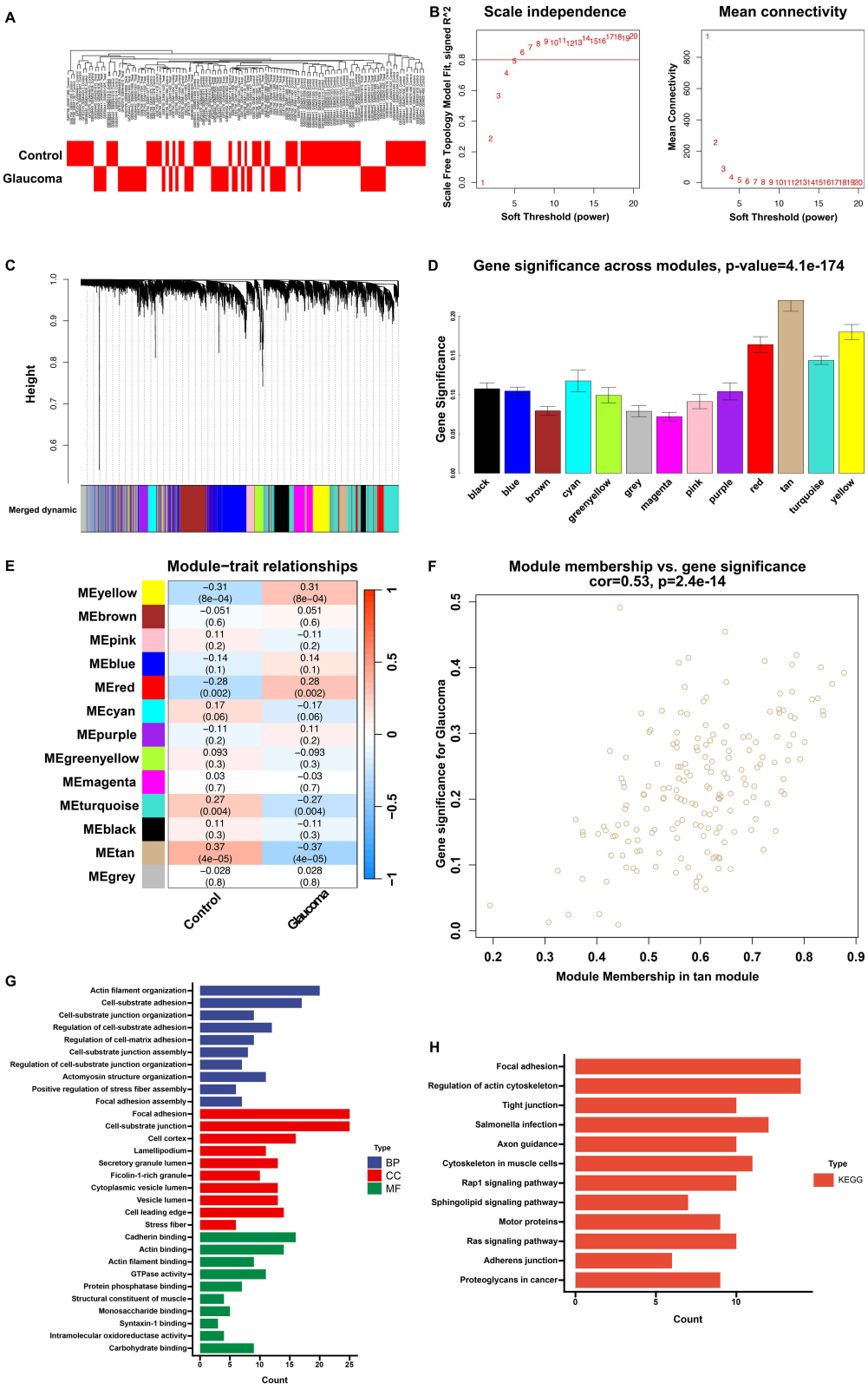

Figure 4 Identification of module gene for glaucoma by weighted gene co-expression network analysis (WGCNA). (**A**) Sample Dendrogram and Trait Heatmap. The upper panel is sample dendrogram which reveals the hierarchical clustering of samples based on their similarity in trait expression profiles. The heatmap below represents the expression levels of specific traits across different samples. Red represents up-regulation and white represents down-regulation; (**B**) Choosing the best soft-threshold power; (**C**) Gene dendrogram and module colors. The dendrogram illustrates the hierarchical clustering of genes based on their expression patterns. The associated color bar at the bottom represents different gene modules identified through dynamic merging, with each color corresponding to a distinct module; (**D**) 13 modules revealed by the WGCNA. (**E**) Heatmap of Pearson correlation of 13 gene module features with glaucoma and normal features. Color corresponds to the size of the correlation. (**F**) Scatter plot of the correlation between genes in the tan module and gene significance for glaucoma. (**G**) GO enrichment analysis of genes in tan module; (**H**) KEGG enrichment analysis of genes in tan module.

https://doi.org/10.2147/IJGM.S545553

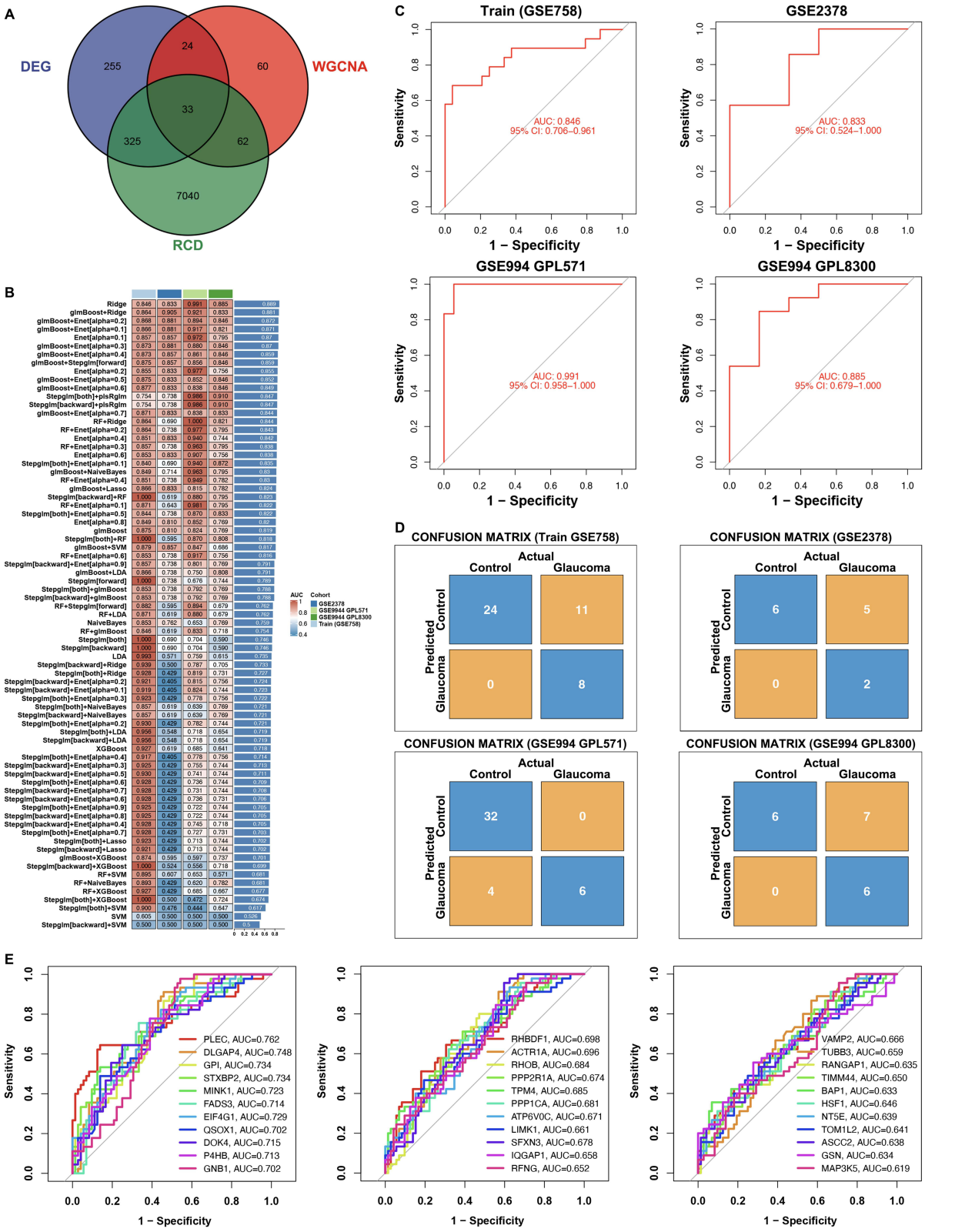

Figure 5 Hub genes and machine-learning to screen out potential predictors. (**A**) Hub genes: intersection of genes identified by DEGs, RCD and WGCNA (tan module); (**B**) Comparison of model performance metrics. AUC values are presented for various machine learning models applied to different cohorts. Ridge is the most effective machine-learning model for glaucoma. Training data was obtained from GSE758, and testing data was obtained from GSE2378, GSE9944 GPL571and GSE9944 GPL8300; (**C**) Receiver operating characteristic (ROC) curve for datasets; (**D**) Confusion matrix for datasets; (**E**) ROC curve for hub genes in machine-learning model Ridge.

dataset (GSE758), indicating strong predictive performance. The validation cohorts (GSE2378:0.833, GSE9944 (GLP571): 0.991, and GSE9944(GLP8300): 0.885) showed similar results (Figure 5C). Glaucoma and control cases are shown in each dataset (Figure 5D). Furthermore, the diagnostic efficacy of the 33-hub gene model and the individual gene models was evaluated using ROC curves, as shown in Figure 5E. The top three genes with the highest ROC values, indicating superior diagnostic or therapeutic potential, were *PLEC, DLGAP4*, and *Glycosylphosphatidylinositol (GPI)*.

Gene Set Enrichment Analysis (GSEA)

Using R packages, we visualized the expression of the three hub genes with the highest AUC values in patients with glaucoma and controls using a violin plot. The expression levels of PLEC, DLGAP4, and GPI in glaucoma patients were downregulated (Figure 6A–C). Using GSEA, we explored the molecular mechanisms underlying glaucoma progression by identifying the specific signaling pathways enriched by the three key hub genes. The pathways enriched in PLEC by GSEA of KEGG analysis included focal adhesion, the MAPK signaling pathway, and oxidative phosphorylation (Figure 6D). The pathways enriched with DLGAP4 by KEGG analysis included regulation of the actin cytoskeleton, cell adhesion, and proteasomes e (Figure 6E). The pathways enriched with GPI by KEGG analysis included the metabolism of butanoate, cytochrome P450, fatty acids, and pyruvate (Figure 6F).

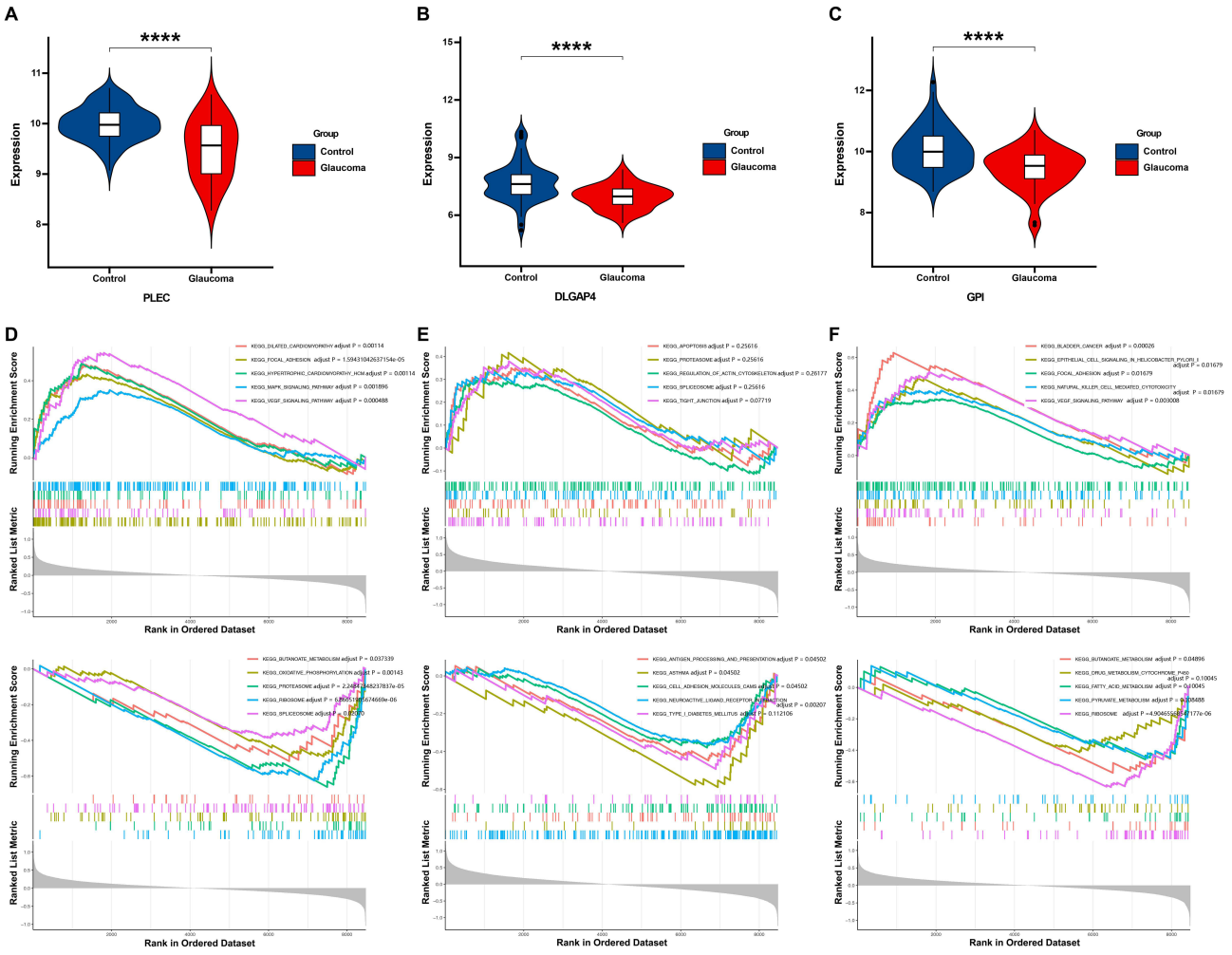

Figure 6 Gene set enrichment analysis (GSEA). (**A–C**) Violin plots of *PLEC, DLGAP4* and *GPI* gene expression levels in glaucoma and non-glaucoma (control) group, ****$P <$ 0.0001 versus control; (**D–F**) GSEA analysis of *PLEC, DLGAP4* and *GPI*. The upper panel shows the results enriched in high expression group. The lower panel shows the results enriched in low expression group.

https://doi.org/10.2147/IJGM.S545553

Immune Cell Infiltration Landscape in Glaucoma Patients

Immune cell infiltration is an emerging driver of RGC damage in the glaucoma pathogenesis.[20–22] We used CIBERSORT analysis to determine the infiltration levels of the 22 immune cell types across the three datasets. Subsequently, we compared the relative abundance of each immune cell type using Wilcoxon test. The results showed the proportion of immune cells in each patient and the correlation between immune cells (Figure 7A). T cells, CD4 naïve and NK cells activated exhibited a statistically significant difference between glaucoma patients and controls (Figure 7B and C).

We further explored the relationship between key genes and immune cells. To investigate PLEC's impact of PLECs on the 22 immune cell types, we used dumbbell plots and correlation scatter plots to display the correlation between immune cells and feature genes. M0 macrophages (p=0.0013) showed a significant positive correlation with PLEC, whereas eosinophils (p=0.038) were significantly negatively correlated (Figure 7D and E). In addition, we determined the Spearman correlation between the 22 immune cell types and the top three genes with the largest AUC values (*PLEC, DLGAP4* and *GPI*) (Figure 7F). These results confirmed that these hub genes are closely related to the level of immune cell infiltration and may play an important role in the immune microenvironment.

Molecular Docking

To investigate the gene-drug network of hub genes for the potential treatment of glaucoma, we conducted a molecular docking analysis to identify possible therapeutic drugs. In our study, we selected *PLEC, DLGAP4* and *GPI* as glaucoma druggable gene sets and selected the top six scoring compounds. We then downloaded the structure of the plectin protein encoded by *PLEC* and obtained the molecular structures of the six compounds (cytochalasin-d, bifonazole, levcromakalim, vinorelbine, tranilast, and RS-56812). Finally, we obtained a molecular docking graph of plectin and the six potential components (Figure 8A–F).

The Protein Level of Retinal PLEC in Glaucoma Mice Group

Using immunofluorescence, we attempted to confirm whether the expression level of PLEC differed between glaucomatous mice and controls in the retina and optic nerve head. PLEC was primarily expressed in ganglion cells, retinal neuron fiber layers, and the optic nerve, as shown in representative images (Figure 9A). Compared to the control, it was significantly decreased in the DBA/2J glaucoma mouse group (Figure 9A and B). This trend was consistent with our GSEA analysis of glaucoma patients (Figure 6A), suggesting that targeting PLEC expression may slow the pathological progression of glaucoma.

Discussion

Currently, almost half of glaucoma patients have intraocular pressure in the normal range, and no available treatment can restore vision loss from glaucoma.[2,23] Thus, understanding the molecular mechanisms driving glaucoma development and developing novel neuroprotective treatments are crucial for improving clinical outcomes. To the best of our knowledge, this is the first study on the contribution of RCD to glaucoma pathogenesis using machine learning, infiltrated immune cell profiling, and molecular docking analysis. Using WGCNA, we identified 33 genes differentially expressed between patients with glaucoma and controls that were also associated with RCD. These 33 hub genes, identified using 75 distinct machine learning approaches, are considered crucial in the genetic underpinnings of glaucoma pathogenesis, as evidenced by their consistent importance across the training and validation cohorts. Molecular docking analysis showed that the top three hub genes with the largest AUC values (PLEC, DLGAP4, and GPI) were promising drugs. These findings suggest novel targets for the detection and treatment of glaucoma.

Neuroinflammation is increasingly being recognized as a critical pathogenic event in glaucoma. Previous studies have mainly focused on glial and Müller cells.[24–26] Our previous work also verified that targeting overactivated microglia attenuates RGC loss through different signaling pathways.[27–29] Emerging evidence has implicated infiltrating immune cells in neurodegenerative cascades. Peng et al established that CD4+ T cells were recruited to the retina and mediated retinal neuron degeneration in experimental colitis in mice.[30] They subsequently identified that T cells from glaucoma patients displayed enhanced activation and a bias towards T helper (Th) 1 responses, and that the infiltration of Th1 cells

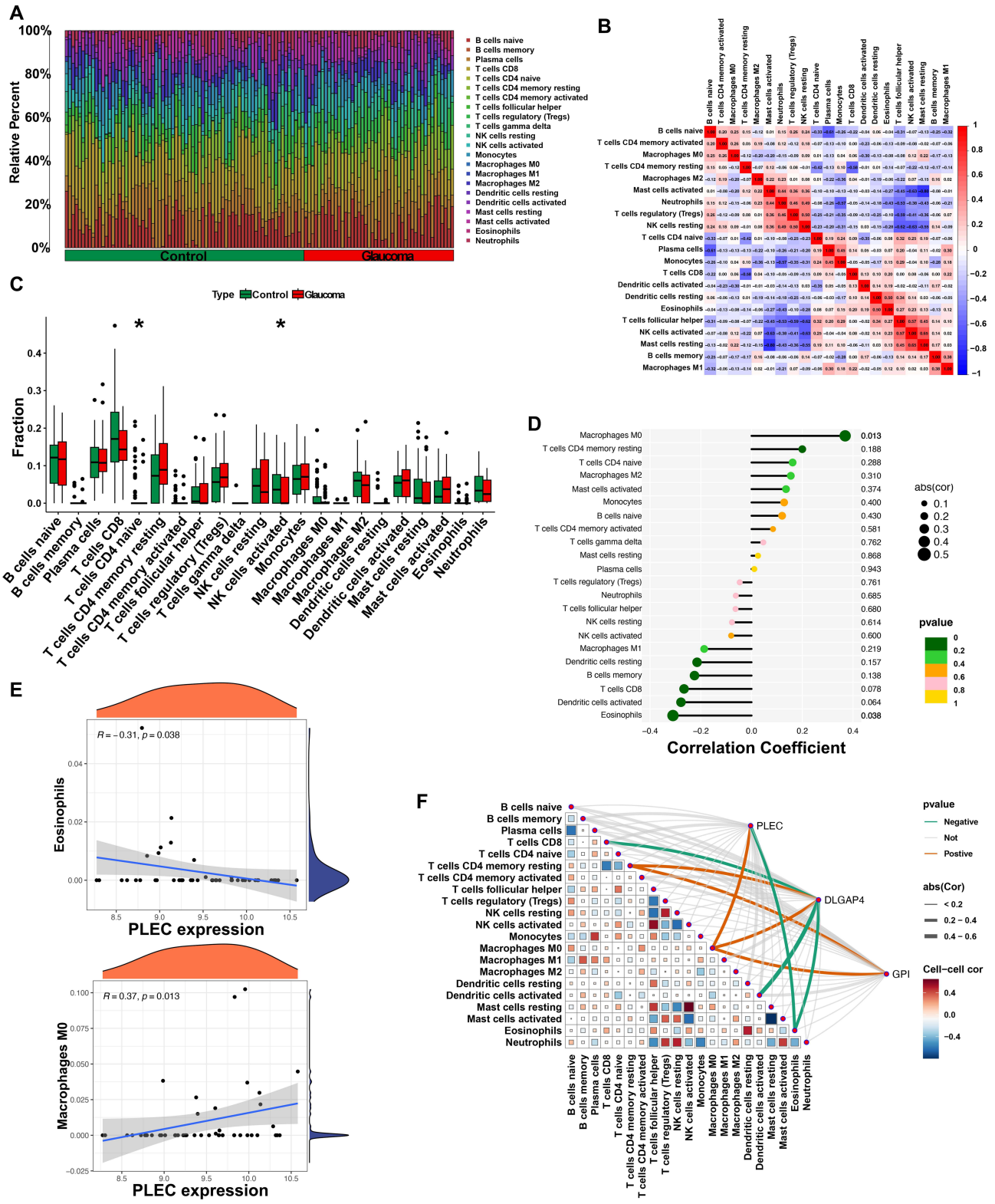

Figure 7 Immune Function Correlation Analysis. (**A**) Immune cell infiltration and percentage in glaucoma patients and non-glaucoma (control) patients; (**B**) Correlation matrix showing relationships between various immune cell types; (**C**) Comparison of immune cell type fractions between glaucoma patients and controls, *$P < 0.05$ versus control; (**D**) Correlation analysis of various immune cell types with glaucoma, dark green ($0 < p$ value ≤ 0.2), green ($0.2 < p$ value ≤ 0.4), Orange ($0.4 < p$ value ≤ 0.6) pink ($0.6 < p$ value ≤ 0.8) yellow ($0.8 < p$ value ≤ 1); (**E**) Correlation analysis between PLEC expression and eosinophils or macrophage M0; (**F**) The relationships between different immune cell type and top 3 hub genes (*PLEC*, *DLGAP4* and *GPI*) for glaucoma.

https://doi.org/10.2147/IJGM.S545553

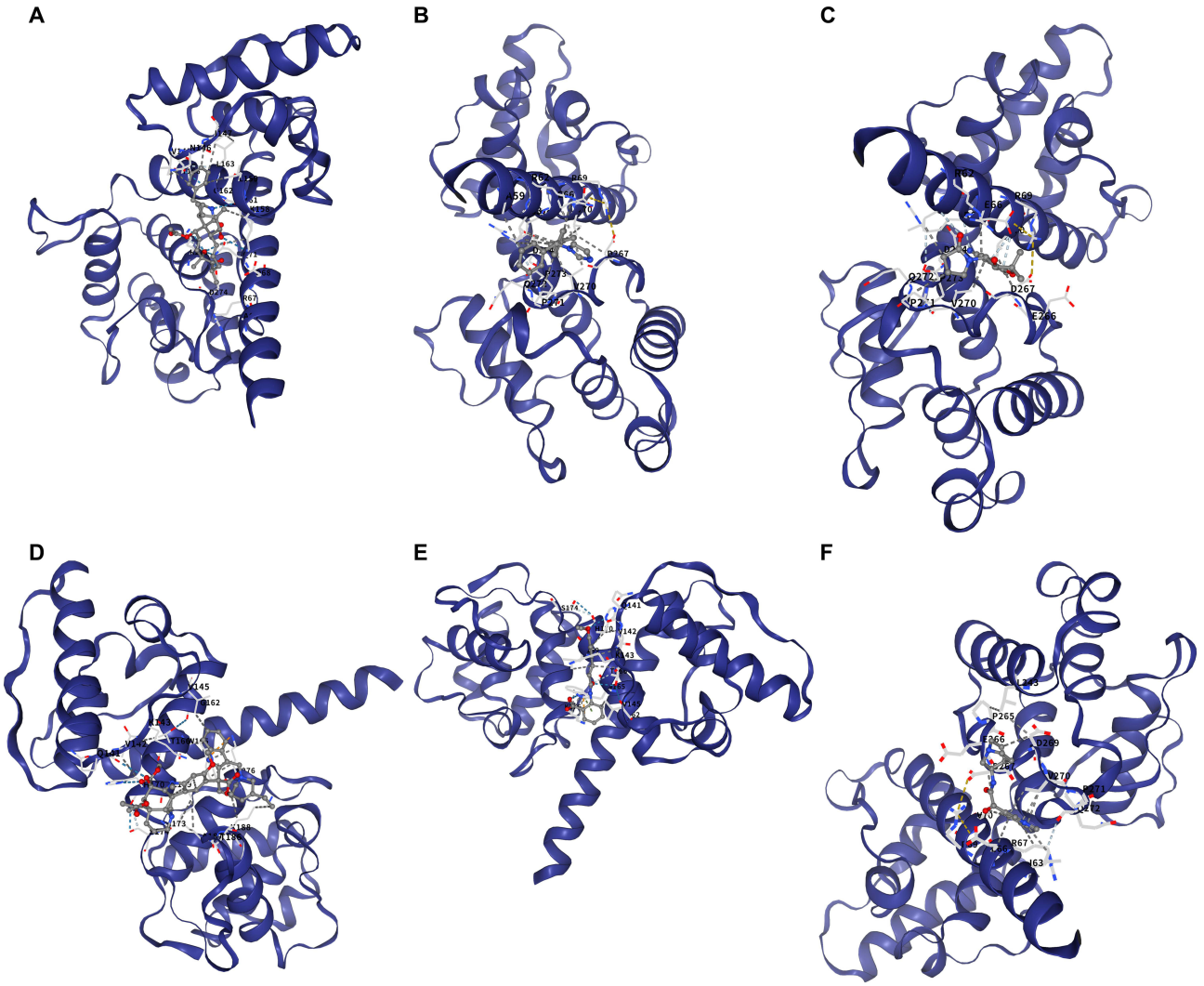

Figure 8 Molecular docking of drug with PLEC, DLGAP4 and GPI Protein. (**A–F**) Figures illustrating the interaction between PLEC protein and compounds including cytochalasin-d, bifonazole, levcromakalim, vinorelbine, tranilast and RS-56812.

into the retina can integrate into the pro-inflammatory glial network.[31] Gramlich et al demonstrated that T cell-deficient *Rag1−/−* knockout mice are significantly protected from glaucomatous RGC loss. In this model, lymphocyte activity contributes to approximately half of all RGC loss in eyes with elevated IOP and normotensive contralateral eyes.[32] Our CIBERSORT analysis revealed significant alterations in T cells CD4 naïve and NK cells in human glaucoma patients and controls. However, the precise characterization of infiltrating immune cell subpopulations and their spatiotemporal dynamics in glaucomatous neurodegeneration remains poorly defined. Further mechanistic investigations are required to elucidate the pathogenic cascade that may reveal novel druggable targets for developing glaucoma-modifying interventions.

PLEC ranked first among the 33 hub genes for pathological alterations in glaucoma using machine learning algorithms. It encodes plectin, a large cytoskeletal protein responsible for regulating signals from the extracellular environment to the nucleus, thereby allowing cells to react to external mechanical stimuli and forces.[33–35] In this study, we observed significantly different expression levels of plectin in the retina and optic nerve head between the DAB/2J mouse glaucoma model and control. Plectin is reported to be expressed in the majority of astrocytes; thus, researchers have proposed that it plays important roles in a number of astrocyte processes, including regulating cell migration, ion and water homeostasis, and modulating synaptic plasticity.[36–39] By utilizing plectin-deficient astrocytes, Žugec et al discovered that the absence of plectin leads to the collective migration of astrocytes and decreases the dynamics of

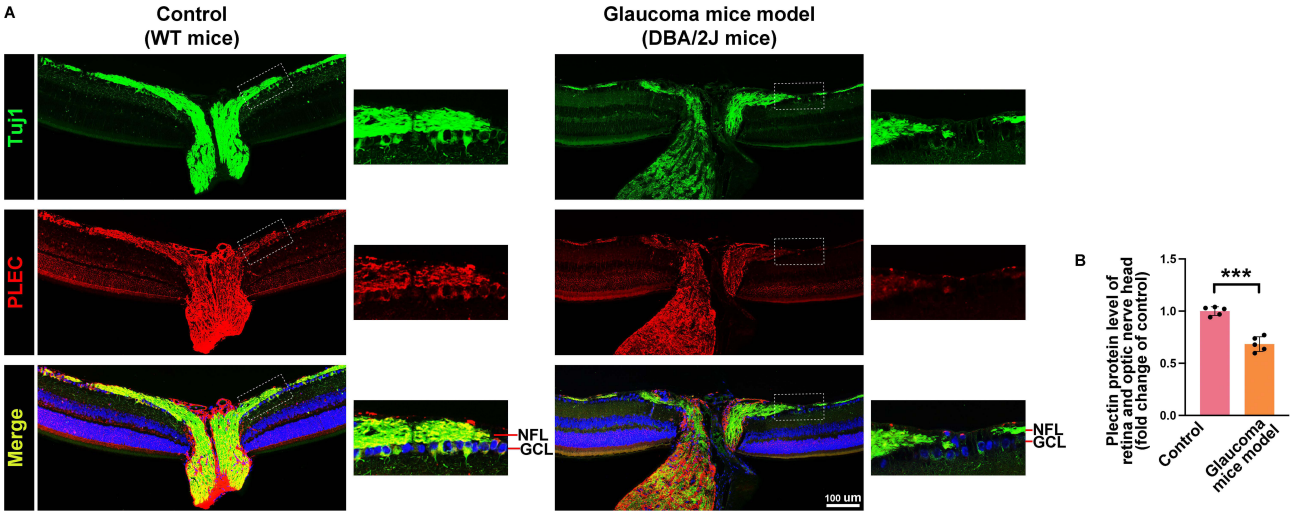

Figure 9 PLEC expression level in mice model of glaucoma. (**A**) Representative images of immunofluorescence staining of anti-Tuji1 and anti-plectin in DAB/2J mice and control. The dashed rectangle boxes display the immunofluorescence staining in the retinal ganglion cell layer (GCL) and retinal nerve fiber layer (NFL); (**B**) Plectin decreased significantly in DAB/2J mice compared to control, ***$P < 0.001$ versus control.

cytoplasmic volume changes in peripheral cell regions.[35] Astrocytes residing in the mammalian retina play crucial roles in maintaining retinal homeostasis and modulating neuron degeneration.[40,41] Despite their functional significance, the expression patterns and functional significance of the cytolinker protein plectin in retinal astrocytes, particularly in glaucoma pathogenesis, remain unexplored . We speculated that PLEC potentially link their cytoskeletal regulatory functions to axonal transport deficits and ONH remodeling. Future investigations should focus on delineating PLEC functions in glaucomatous neurodegeneration.

Among the 33 hub genes identified, *DLGAP5* and *GPI* ranked second and third, respectively, as indicated by bioinformatics analysis. The family of Discs large associated proteins (DLGAPs) are important scaffold proteins in postsynaptic density (PSD) and are expressed in the synaptic terminals of postsynaptic neurons.[42] DLGAP4 is also required for the organization of glial cell adherens junction components and actin cytoskeleton dynamics at the apical domain, as well as during neuronal migration.[43] Our previous study confirmed synaptic loss and axonal transport deficits in a mouse model of glaucoma.[28,44] However, there is currently no research focusing on the involvement of DLGAP4 in synaptic remodeling and neuroinflammatory glial activation in glaucoma pathobiology. GPI is a glycol-lipid that anchors several proteins to the cell surface and serves as a critical signaling nexus through interactions with G protein-coupled receptors and lipid raft-associated kinases.[45] GPI-anchor proteins and pathways are crucial for numerous biological processes through interactions with signaling effectors at the cell surface, and they are fundamental in early neurogenesis and neural development by shaping the properties of various types of synapses and circuits.[45–47] Still. However, little is known about the role of GPI in the pathology of glaucoma. Further experiments are needed to clarify the roles of DLGAP and GPI in glaucoma.

Conclusion

In conclusion, through analysis of RCD pathways in glaucomatous neurodegeneration, this study delineated a molecular network comprising 33 hub genes combined with the WGCNA method. These genes were further validated as crucial to the pathogenesis of glaucoma using 75 separate machine-learning algorithms. Among these genes, *PLEC* (a cytoskeletal remodeling regulator), *DLGAP4* and *GPI (*synaptic plasticity modifier) are strong candidates for glaucomatous neuropathy, with possible drugs based on molecular docking analysis. Furthermore, infiltrated immune cells were observed, suggesting potential immune-related mechanisms involved in glaucoma pathogenesis. However, further experiments are required to validate the roles and mechanisms of these genes in immune cells. In summary, our study identified new targets for the detection and treatment of glaucoma.

Abbreviations

RCD, regulated cell death; DEGs, differentially expressed genes; WGCNA, Weighted Gene Co-Expression Network Analysis; GSEA, Gene set enrichment analysis; GPI, Glycosylphosphatidylinositol; RGCs, retinal ganglion cells; ACD, accidental cell death; PCD, programmed cell death; GO, Gene Ontology; KEGG, Kyoto Encyclopedia of Genes and Genomes.

Data Sharing Statement

The datasets generated and/or analyzed during the current study are available from the corresponding author upon reasonable request.

Ethical Approval

This study was conducted in accordance with the principles of the Declaration of Helsinki. Approval was granted by the Ethics Committee of Huazhong University of Science and Technology.

Consent for Publication

All authors have provided full consent for the publication of the present article.

Funding

This study was supported by the National Natural Science Foundation of China (grant number: 82201183).

Disclosure

The authors declare that they have no competing financial interests or personal relationships that could have influenced the work reported in this study.

References

1. Tham YC, Li X, Wong TY, Quigley HA, Aung T, Cheng CY. Global prevalence of glaucoma and projections of glaucoma burden through 2040: a systematic review and meta-analysis. *Ophthalmology*. 2014;121(11):2081–2090. doi:10.1016/j.ophtha.2014.05.013
2. Jayaram H, Kolko M, Friedman DS, Gazzard G. Glaucoma: now and beyond. *Lancet*. 2023;402(10414):1788–1801. doi:10.1016/S0140-6736(23)01289-8
3. Weinreb RN, Aung T, Medeiros FA. The pathophysiology and treatment of glaucoma: a review. *JAMA*. 2014;311(18):1901–1911. doi:10.1001/jama.2014.3192
4. Almasieh M, Wilson AM, Morquette B, Cueva Vargas JL, Di Polo A. The molecular basis of retinal ganglion cell death in glaucoma. *Prog Retin Eye Res*. 2012;31(2):152–181.
5. Tang D, Kang R, Berghe TV, Vandenabeele P, Kroemer G. The molecular machinery of regulated cell death. *Cell Res*. 2019;29(5):347–364. doi:10.1038/s41422-019-0164-5
6. Galluzzi L, Bravo-San Pedro JM, Vitale I, et al. Essential versus accessory aspects of cell death: recommendations of the NCCD 2015. *Cell Death Differ*. 2015;22(1):58–73. doi:10.1038/cdd.2014.137
7. Shen S, Ji C, Wei K. Cellular senescence and regulated cell death of tubular epithelial cells in diabetic kidney disease. *Front Endocrinol*. 2022;13:924299. doi:10.3389/fendo.2022.924299
8. Ren L, Zhang Q, Zhou J, Wang X, Zhu D, Chen X. Leveraging diverse regulated cell death patterns to identify diagnosis biomarkers for Alzheimer's disease. *J Prev Alzheimers Dis*. 2024;11(6):1775–1788. doi:10.14283/jpad.2024.119
9. Zhang W, Zhu Y, Liu H, et al. Pan-cancer evaluation of regulated cell death to predict overall survival and immune checkpoint inhibitor response. *NPJ Precis Oncol*. 2024;8(1):77. doi:10.1038/s41698-024-00570-5
10. Doerflinger M, Deng Y, Whitney P, et al. Flexible usage and interconnectivity of diverse cell death pathways protect against intracellular infection. *Immunity*. 2020;53(3):533–47e7. doi:10.1016/j.immuni.2020.07.004
11. Gong L, Huang D, Shi Y, Liang Z, Bu H. Regulated cell death in cancer: from pathogenesis to treatment. *Chin Med J*. 2023;136(6):653–665. doi:10.1097/CM9.0000000000002239
12. Wang Y, Kanneganti TD. From pyroptosis, apoptosis and necroptosis to PANoptosis: a mechanistic compendium of programmed cell death pathways. *Comput Struct Biotechnol J*. 2021;19:4641–4657. doi:10.1016/j.csbj.2021.07.038
13. Basavarajappa D, Galindo-Romero C, Gupta V, et al. Signalling pathways and cell death mechanisms in glaucoma: insights into the molecular pathophysiology. *Mol Aspects Med*. 2023;94:101216. doi:10.1016/j.mam.2023.101216
14. Yang Y, Sun X. Retinal ganglion cell death in glaucoma: advances and caveats. *Curr Eye Res*. 2023;48(1):1–10. doi:10.1080/02713683.2022.2068182
15. Qin Q, Yu N, Gu Y, et al. Inhibiting multiple forms of cell death optimizes ganglion cells survival after retinal ischemia reperfusion injury. *Cell Death Dis*. 2022;13(5):507. doi:10.1038/s41419-022-04911-9

16. Hu J, Luo Y, Wang X. Multi-omics analysis of druggable genes to facilitate Alzheimer's disease therapy: a multi-cohort machine learning study. *J Prev Alzheimers Dis*. 2025;12:100128. doi:10.1016/j.tjpad.2025.100128
17. Shi S, Huang C, Tang X, Liu H, Feng W, Chen C. Identification and verification of diagnostic biomarkers for deep infiltrating endometriosis based on machine learning algorithms. *J Biol Eng*. 2024;18(1):70. doi:10.1186/s13036-024-00466-9
18. Xia J, Wishart DS. MSEA: a web-based tool to identify biologically meaningful patterns in quantitative metabolomic data. *Nucleic Acids Res*. 2010;38(Web Server issue):W71–7. doi:10.1093/nar/gkq329
19. Chen B, Khodadoust MS, Liu CL, Newman AM, Alizadeh AA. Profiling tumor infiltrating immune cells with CIBERSORT. *Methods Mol Biol*. 2018;1711:243–259.
20. He C, Xiu W, Chen Q, et al. Gut-licensed beta7(+) CD4(+) T cells contribute to progressive retinal ganglion cell damage in glaucoma. *Sci Transl Med*. 2023;15(707):eadg1656. doi:10.1126/scitranslmed.adg1656
21. Williams PA, Braine CE, Kizhatil K, et al. Inhibition of monocyte-like cell extravasation protects from neurodegeneration in DBA/2J glaucoma. *Mol Neurodegener*. 2019;14(1):6. doi:10.1186/s13024-018-0303-3
22. Xu Z, Ma Y, Li J, et al. Microglial phagocytosis involves hyperoxia-induced vessel regression in the neonatal retina. *Visual Neuroscience*. 2025;42:e004. doi:10.48130/vns-0025-0004
23. Wang D, Huang W, Li Y, et al. Intraocular pressure, central corneal thickness, and glaucoma in Chinese adults: the liwan eye study. *Am J Ophthalmol*. 2011;152(3):454–62e1. doi:10.1016/j.ajo.2011.03.005
24. Liu YX, Sun H, Guo WY. Astrocyte polarization in glaucoma: a new opportunity. *Neural Regen Res*. 2022;17(12):2582–2588. doi:10.4103/1673-5374.339470
25. Quaranta L, Bruttini C, Micheletti E, et al. Glaucoma and neuroinflammation: an overview. *Surv Ophthalmol*. 2021;66(5):693–713. doi:10.1016/j.survophthal.2021.02.003
26. Williams PA, Marsh-Armstrong N, Howell GR, Lasker I. Neuroinflammation in glaucoma: a new opportunity. *Exp Eye Res*. 2017;157:20–27. doi:10.1016/j.exer.2017.02.014
27. Yao K, Liang X, Zhang G, et al. Covalent Organic Framework (COF): a drug and carrier to attenuate retinal ganglion cells death in an acute glaucoma mouse model. *Polymers*. 2022;14(16):3265. doi:10.3390/polym14163265
28. Yao K, Mou Q, Lou X, et al. Microglial SIRT1 activation attenuates synapse loss in retinal inner plexiform layer via mTORC1 inhibition. *J Neuroinflammation*. 2023;20(1):202. doi:10.1186/s12974-023-02886-8
29. Yao K, Zhao Y, Jin P, et al. Involvement of the NLRC4 inflammasome in promoting retinal ganglion cell death in an acute glaucoma mouse model. *Exp Eye Res*. 2021;203:108388. doi:10.1016/j.exer.2020.108388
30. Peng K, Xiao J, Wang J, et al. MAdCAM-1 mediates retinal neuron degeneration in experimental colitis through recruiting gut-homing CD4(+) T cells. *Mucosal Immunol*. 2021;14(1):152–163. doi:10.1038/s41385-020-0282-x
31. He C, Peng K, Zhu X, et al. Th1 cells contribute to retinal ganglion cell loss in glaucoma in a VCAM-1-dependent manner. *J Neuroinflammation*. 2024;21(1):43. doi:10.1186/s12974-024-03035-5
32. Gramlich OW, Godwin CR, Heuss ND, Gregerson DS, Kuehn MH. T and B lymphocyte deficiency in Rag1-/- mice reduces retinal ganglion cell loss in experimental glaucoma. *Invest Ophthalmol Vis Sci*. 2020;61(14):18. doi:10.1167/iovs.61.14.18
33. Goldmann WH. Intermediate filaments and cellular mechanics. *Cell Biol Int*. 2018;42(2):132–138. doi:10.1002/cbin.10879
34. Sorial AK, Hofer IMJ, Tselepi M, et al. Multi-tissue epigenetic analysis of the osteoarthritis susceptibility locus mapping to the plectin gene PLEC. *Osteoarthritis Cartilage*. 2020;28(11):1448–1458. doi:10.1016/j.joca.2020.06.001
35. Zugec M, Furlani B, Castanon MJ, et al. Plectin plays a role in the migration and volume regulation of astrocytes: a potential biomarker of glioblastoma. *J Biomed Sci*. 2024;31(1):14. doi:10.1186/s12929-024-01002-z
36. Fuchs P, Zorer M, Reipert S, et al. Targeted inactivation of a developmentally regulated neural plectin isoform (plectin 1c) in mice leads to reduced motor nerve conduction velocity. *J Biol Chem*. 2009;284(39):26502–26509. doi:10.1074/jbc.M109.018150
37. Lie AA, Schroder R, Blumcke I, Magin TM, Wiestler OD, Elger CE. Plectin in the human central nervous system: predominant expression at pia/glia and endothelia/glia interfaces. *Acta Neuropathol*. 1998;96(3):215–221. doi:10.1007/s004010050885
38. Potokar M, Jorgacevski J. Plectin in the central nervous system and a putative role in brain astrocytes. *Cells*. 2021;10(9):2353. doi:10.3390/cells10092353
39. Prechova M, Adamova Z, Schweizer AL, et al. Plectin-mediated cytoskeletal crosstalk controls cell tension and cohesion in epithelial sheets. *J Cell Biol*. 2022;221(3). doi:10.1083/jcb.202105146
40. Cameron EG, Nahmou M, Toth AB, et al. A molecular switch for neuroprotective astrocyte reactivity. *Nature*. 2024;626(7999):574–582. doi:10.1038/s41586-023-06935-3
41. Vecino E, Rodriguez FD, Ruzafa N, Pereiro X, Sharma SC. Glia-neuron interactions in the mammalian retina. *Prog Retin Eye Res*. 2016;51:1–40. doi:10.1016/j.preteyeres.2015.06.003
42. Rasmussen AH, Rasmussen HB, Silahtaroglu A. The DLGAP family: neuronal expression, function and role in brain disorders. *Mol Brain*. 2017;10(1):43. doi:10.1186/s13041-017-0324-9
43. Romero DM, Poirier K, Belvindrah R, et al. Novel role of the synaptic scaffold protein Dlgap4 in ventricular surface integrity and neuronal migration during cortical development. *Nat Commun*. 2022;13(1):2746. doi:10.1038/s41467-022-30443-z
44. Ye M, Huang J, Mou Q, et al. CD82 protects against glaucomatous axonal transport deficits via mTORC1 activation in mice. *Cell Death Dis*. 2021;12(12):1149. doi:10.1038/s41419-021-04445-6
45. Um JW, Ko J. Neural glycosylphosphatidylinositol-anchored proteins in synaptic specification. *Trends Cell Biol*. 2017;27(12):931–945. doi:10.1016/j.tcb.2017.06.007
46. Borza R, Matas-Rico E, Perrakis A, Moolenaar WH. Unlocking the signaling potential of GPI-anchored proteins through lipolytic cleavage. *Trends Cell Biol*. 2025;35(9):732–744. doi:10.1016/j.tcb.2024.12.010
47. Thorpe HJ, Pedersen BS, Dietze M, et al. Identification of CNTN2 as a genetic modifier of PIGA-CDG in a family with incomplete penetrance and in drosophila. *Am J Hum Genet*. 2025;112(3):572–582. doi:10.1016/j.ajhg.2025.01.017

International Journal of General Medicine

Dovepress
Taylor & Francis Group

Publish your work in this journal

The International Journal of General Medicine is an international, peer-reviewed open-access journal that focuses on general and internal medicine, pathogenesis, epidemiology, diagnosis, monitoring and treatment protocols. The journal is characterized by the rapid reporting of reviews, original research and clinical studies across all disease areas. The manuscript management system is completely online and includes a very quick and fair peer-review system, which is all easy to use. Visit http://www.dovepress.com/testimonials.php to read real quotes from published authors.

Submit your manuscript here: https://www.dovepress.com/international-journal-of-general-medicine-journal